

This is the accepted manuscript made available via CHORUS. The article has been published as:

## Configurations and decay hindrances of high-K states in $^{180}\text{Hf}$

S. K. Tandel, P. Chowdhury, F. G. Kondev, R. V. F. Janssens, T. L. Khoo, M. P. Carpenter, T. Lauritsen, C. J. Lister, D. Seweryniak, S. Zhu, A. Deacon, S. J. Freeman, N. J. Hammond, G. D. Jones, E. F. Moore, and J. F. Smith

Phys. Rev. C **94**, 064304 — Published 2 December 2016

DOI: [10.1103/PhysRevC.94.064304](https://doi.org/10.1103/PhysRevC.94.064304)

# Configurations and decay hindrances of high- $K$ states in $^{180}\text{Hf}$

S.K. Tandel,<sup>1,2</sup> P. Chowdhury,<sup>1</sup> F.G. Kondev,<sup>3</sup> R.V.F. Janssens,<sup>3</sup> T.L. Khoo,<sup>3</sup> M.P. Carpenter,<sup>3</sup> T. Lauritsen,<sup>3</sup> C.J. Lister,<sup>1,3</sup> D. Seweryniak,<sup>3</sup> S. Zhu,<sup>3</sup> A. Deacon,<sup>4</sup> S.J. Freeman,<sup>4</sup> N.J. Hammond<sup>a,3</sup> G.D. Jones,<sup>5</sup> E.F. Moore,<sup>3</sup> and J.F. Smith<sup>b4</sup>

<sup>1</sup>*Department of Physics, University of Massachusetts*

*Lowell, Lowell, Massachusetts 01854, USA*

<sup>2</sup>*UM-DAE Centre for Excellence in Basic Sciences, Mumbai 400098, India*

<sup>3</sup>*Argonne National Laboratory, Argonne, Illinois 60439, USA*

<sup>4</sup>*University of Manchester, Manchester M13 9PL, UK*

<sup>5</sup>*University of Liverpool, Liverpool L69 7ZE, UK*

(Dated: November 21, 2016)

## Abstract

Multi-quasiparticle high- $K$  states, several of which are isomeric, were observed in  $^{180}\text{Hf}$  with the Gammasphere array. Lifetimes in the  $ns - \mu s$  range were determined using centroid-shift and decay measurements within a  $\mu s$  coincidence time window. The configurations of high- $K$  states involve two and four quasiparticles, with states up to  $K^\pi=(18^-)$  established. High- $K$  excitations are found to be progressively more favored with increasing excitation energy. The  $K$  quantum number is quite robust up to the highest spins observed, as evidenced by the large values of the reduced hindrance for isomeric decays. Rotational bands built on three high- $K$  states are identified, and the measured branching ratios in these sequences enable the assignment of underlying configurations. Multi-quasiparticle calculations using the Lipkin-Nogami approach for pairing, with blocking included, reproduce the observed high- $K$  energies quite well.

PACS numbers: 21.10.Re, 21.60.Ev, 23.20.Lv, 27.90.+b

---

<sup>a</sup> Present address: Cambridge University Press, Cambridge CB2 8RU, UK

<sup>b</sup> Present address: University of the West of Scotland, Paisley, PA1 2BE Scotland, UK

## I. INTRODUCTION

Deformed, mid-shell nuclei in the  $A \approx 180$  region are characterized by both protons and neutrons occupying high- $\Omega$  orbitals located near the Fermi surface. A natural consequence is the presence of intrinsic high- $K$  states which can favorably compete for yrast status with collective excitations. The observation of intrinsic states, especially  $K$  isomers, and the associated rotational bands can provide insight into the relative positions of the underlying single-particle orbitals for which there is limited information in neutron-rich territory. While  $K$  isomers at high spin have been identified in many nuclei in this region; *e.g.* [1–6], isotopes of Hf are particularly well suited for such studies since they are considered to be some of the best examples of rigid, axially-symmetric, prolate rotors. As a result,  $K$  is a relatively “good” quantum number in these systems. This work is focused on  $^{180}\text{Hf}$ , the heaviest stable Hf isotope.

There are several experimental challenges in  $K$ -isomer measurements. Quite often, there is more than one decay branch from a given long-lived state. For a complete understanding, it is crucial to identify all the decay branches from an isomer. A precise determination of half-lives, which may range from  $> 1\text{ ns}$  to years, is essential as well. Further, there may be situations involving multiple isomers, feeding into one another. In such cases, it is imperative to appropriately deconvolute the decay curves from the deexcitation of the various long-lived levels. Typically, measurements in several time regimes may be required to study different  $K$  isomers in the same nucleus. For long-lived ( $T_{1/2} \gg 1\text{ }\mu\text{s}$ ) ones, identification of  $\gamma$  rays feeding and deexciting the isomer is necessary. Unambiguous assignment of distinct rotational sequences to specific isomeric states is required. Realizing all the above conditions in a single experiment is typically quite challenging and sometimes not feasible. As a result, multiple measurements, each focused on a specific aspect, may be required.

There are several previous measurements of excited states in  $^{180}\text{Hf}$ . The low-lying  $K^\pi=8^-$  isomer, with a  $5.5\text{ h}$  half-life, was first identified more than sixty years ago at Argonne National Laboratory [7]. About fifty years later, several other high-spin isomers were reported [8]. The present work, also performed at the same laboratory, extends the number of  $K$  isomers established in  $^{180}\text{Hf}$  to five. A few other high- $K$  states were identified as well. Half-lives, or limits thereof, were newly determined for three states; these could not be determined for other levels. In the earlier work [8], experimental parameters had been optimized for isomers

with  $T_{1/2} \gg 1 \mu s$ , whereas the present study is focused on sub-microsecond ones.

## II. EXPERIMENT AND DATA ANALYSIS

Excited states in  $^{180}\text{Hf}$  were studied through deep-inelastic reactions, with a 1.4-GeV  $^{207}\text{Pb}$  beam from the ATLAS accelerator at Argonne National Laboratory, incident on an isotopically-enriched, 250 mg/cm<sup>2</sup>  $^{180}\text{Hf}$  target. The beam energy was chosen to be  $\approx 8\%$  above the Coulomb barrier. The Gammasphere array [9, 10], comprising of 100 Compton-suppressed Ge detectors, was used to record coincidence events in two time regimes. Prompt events were recorded with the beam hitting the target, with the natural 82.5 ns pulsing from ATLAS. So-called pulsed events were measured with a cycle where the beam was on target for 1 ns, followed by a 825-ns off period. These data complement earlier out-of-beam studies focused on long-lived ( $T_{1/2} \gg 1 \mu s$ ) isomers [8], and the prompt spectroscopy of  $^{180}\text{Hf}$  [11, 12] using Gammasphere in conjunction with the auxiliary heavy-ion counter CHICO [13].

## III. RESULTS

High- $K$  states with excitation energies ranging from  $E_x \approx 1.1$  to 3.6 MeV, and spins from  $K^\pi = 4^-$  to  $(18^-)$  are observed (Fig. 1). Rotational bands feeding the  $K^\pi = 10^+$ ,  $11^-$ , and  $14^+$  states are new to this work. Configuration assignments for these structures are based on measured branching ratios in the associated rotational bands. The half-life of the  $K^\pi = 6^+$  state is newly measured, while half-lives of the  $K^\pi = 10^+$  and  $K^\pi = 12^+$  states, and the level at 2535 keV, are revised from previously reported values [8].

The half-life of the  $K^\pi = 4^-$  state is measured to be  $0.52(8) \mu s$  (Fig. 2), consistent with the previously reported value of  $0.57(2) \mu s$  [14]. For the  $K^\pi = 6^+$  state,  $T_{1/2} = 2.8(3) ns$  is obtained using the centroid-shift technique (Figs. 3 and 4). Centroids of measured time distributions for prompt transitions with energies ranging from  $\approx 200$  keV to 1.4 MeV are plotted in Fig. 4. The deviation in the location of the centroid of a distribution for a delayed transition from an isomeric state with respect to that for a prompt transition with similar energy is indicative of the mean life ( $\tau$ ) of the long-lived level [15]. It is evident from Figs. 3 and 4 that the centroid of the 1394-keV transition deexciting the  $K^\pi = 6^+$  state is shifted by  $4.0(4) ns$  with respect to that for a prompt  $\gamma$  ray, implying a half-life of  $2.8(3) ns$ . The

data also allowed for a measurement of the half-life of the  $K^\pi = 17/2^+$  state in  $^{179}\text{Hf}$ . The present data indicate  $T_{1/2}=4.1(4)$  ns (Fig. 4) for this level consistent with the previously reported value of  $3(1)$  ns [16].

The  $K^\pi = 10^+$  state had previously been assigned a half-life of  $15(5)$   $\mu\text{s}$  [8]. In the present work, it is possible to observe prompt coincidence relationships across this state (Fig. 1); *i.e.*, between the 479, 772, and 1040-keV transitions deexciting this level and the ones feeding it. No appreciable shift in the centroid of the time spectra for transitions deexciting this state is visible, indicating that its half-life is short ( $<1\text{-}2$  ns). The  $15\text{-}\mu\text{s}$  half-life previously assigned can, most likely, be attributed to the long-lived feeding from higher-lying  $K$  isomers with  $T_{1/2} \gg 1$   $\mu\text{s}$ . The rotational band built on the  $K^\pi=10^+$  state at 2424 keV is newly identified, with 267-, 288-, 308-, 326- and 344-keV,  $\Delta I=1$  transitions and 555-, 596-, 634- and 670-keV,  $\Delta I=2$  cross-over ones (Fig. 5).

The  $K^\pi = 11^-$  structure is also newly observed and decays to levels in the  $K^\pi = 8^-$  band through the 1118- and 1386-keV transitions. Only five  $\gamma$  rays, with energies 314, 335, 357, 649 and 692 keV could be identified in this sequence (Fig. 5).

The  $K^\pi = 12^+$  state at  $E_x=2484$  keV is observed to deexcite to levels in the  $K^\pi = 8^-$  band through four transitions with multipolarities ranging from  $E1$ , and  $M2$  to  $E3$ . The half-life of the  $12^+$  state was previously reported to be  $10(1)$   $\mu\text{s}$  [8]. This value had been obtained through a two-component fit to the time spectra for transitions deexciting this state. These spectra were obtained in singles mode and were timed with respect to a beam-off trigger. Thus, feeding from multiple higher-lying isomers with longer half-lives could possibly lead to an erroneous assignment of the half-life of the state. In the present work, coincidence events between transitions directly feeding and deexciting the  $12^+$  level have been observed, similar to the case of the  $K^\pi = 4^-$  state. The half-life of the  $K^\pi = 12^+$  state is determined to be  $T_{1/2} = 0.94(11)$   $\mu\text{s}$  (Fig. 6).

The state at  $E_x=2535$  keV had previously been assigned spin-parity  $14^+$  and  $T_{1/2}\gg 10$   $\mu\text{s}$ . The relative intensities of the 137- and 184-keV transitions and of the 270-keV  $\gamma$  ray which feed into the  $12^+$  level at 2484 keV, and the one at 2535 keV, respectively, in spectra gated on transitions below and above the  $K^\pi=12^+$  and  $K^\pi=14^+$  levels are found to be quite similar (Fig. 7). This implies that the half-life of the 2535-keV level is considerably shorter than that of the  $K^\pi=12^+$  state at 2484 keV; *i.e.*,  $T_{1/2} \ll 1$   $\mu\text{s}$  for the 2535-keV level. Direct determination of the half-life of the 2535-keV level state through the observation of

a time difference (as described earlier) is not possible from the present data due to the low energy (52 keV), and consequent reduced detection efficiency, of the transition deexciting this level. The spin-parity of the 2535-keV level had been assigned as  $14^+$  in the previous work [8], based on the argument that the resulting  $K$  hindrance would explain the long half-life. However, on account of the shorter half-life, an  $I^\pi=(13^+)$  assignment, which had been excluded previously, is possible and appears more likely. The state at 2805 keV is assigned  $K^\pi=14^+$ , based on the relative intensity of the observed decays from this state, and branching ratios in the newly identified rotational band built on it (see discussion below). The rotational sequence built on the  $K^\pi=14^+$  state consists of  $\Delta I=1$  transitions with energy 293, 317, 344, 367 and 393 keV, and  $\Delta I=2$  cross-over ones with energy 610, 661, 711 and 760 keV (Fig. 5).

The presence of a long-lived isomer with a spin-parity  $K^\pi=(18^-)$  observed in the previous work [8] is confirmed in the present data. A half-life  $T_{1/2}>1\ \mu s$  is indicated, not inconsistent with the value  $90(10)\ \mu s$  reported earlier [8].

#### IV. DISCUSSION

The rigid prolate shape characteristic of  $^{180}\text{Hf}$ , combined with the presence of several nucleons occupying high- $\Omega$  orbitals near the Fermi surface, favors high- $K$  excitations. These are near-yrast when considering the two- and four-quasiparticle excitations up to angular momentum  $I=12\ \hbar$ . Above  $14\hbar$ , however, the yrast line is dominated by high- $K$  excitations which become energetically favored compared to collective rotation as illustrated in Fig. 8; *e.g.*, the  $K^\pi=(18^-)$  state is more than 1 MeV lower in excitation than the corresponding  $18^+$  collective rotational level. A similar feature is present in several neighboring nuclei as well.

For high- $K$  states, the reduced hindrance is defined as  $f_\nu = F^{1/\nu} = \left[ \frac{T_{1/2}^\gamma}{T_{1/2}^W} \right]^{1/\nu}$ , where  $T_{1/2}^\gamma$  is the partial  $\gamma$ -ray half-life,  $T_{1/2}^W$  is the corresponding Weisskopf estimate, and  $\nu = \Delta K - \lambda$  is the degree of  $K$ -forbiddenness of the transition with  $\lambda$  being the transition multipolarity. For the  $K^\pi=6^+$  state, the reduced hindrance ( $f_\nu$ ) is relatively small ( $\approx 10$ ). For all other high- $K$  states where half-lives are firmly established,  $f_\nu \gg 10$ , indicative of the robustness of the  $K$  symmetry (Table I). This aspect is particularly evident in the decay of the  $K^\pi=12^+$  level where  $E1$ ,  $M2$  and  $E3$  transitions with comparable intensities deexcite the isomer to

the  $K^\pi=8^-$  rotational band.

The  $K^\pi=6^+$  states in even Hf isotopes have an underlying  $\pi^2[404]7/2^+ \otimes [402]5/2^+$  two-quasiproton configuration, with mixing of a two-quasineutron one in  $^{176}\text{Hf}$  [17]. The latter is lowest in energy in  $^{176}\text{Hf}$ , with the longest half-life,  $T_{1/2}=9.6(2) \mu\text{s}$ ; *e.g.*, Ref. [18]. The decrease in reduced hindrance for both proton-rich and neutron-rich isotopes (Fig. 9) may be attributed to increased mixing as the  $K^\pi=6^+$  states move away from the yrast line. A detailed discussion of this aspect may be found in a recent review [19].

Configuration assignments proposed for high- $K$  states are based on the  $g$  factors inferred from branching ratios of  $\Delta I=1$  and  $\Delta I=2$  transitions measured in rotational bands built on these states and on comparisons with values expected for different possible configurations involving nucleons near the proton and neutron Fermi levels.

The quadrupole admixture ( $q$ ) is written in terms of the magnitude of the in-band quadrupole/dipole mixing ratio ( $\delta$ ) as:

$$q = \frac{\delta^2}{1 + \delta^2} = \frac{2K^2(2I - 1)}{(I + 1)(I + K - 1)(I - K - 1)} \left( \frac{E_1}{E_2} \right)^5 \frac{T_2}{T_1} \quad (1)$$

where the subscripts 1,2 refer to  $\Delta I=1,2$  transitions, respectively, and  $E_{1,2}$  are the transition energies with  $T_{1,2}$  being the corresponding intensities and  $I$  the spin of the initial level. The mixing ratio ( $\delta$ ) can be used to estimate the intrinsic  $g$  factor ( $g_K$ ) characteristic of a given high- $K$  band.

The relation between the  $g_K$  and  $g_R$  intrinsic and rotational  $g$  factors, and mixing ratio  $\delta$ , is given by:

$$\left| \frac{g_K - g_R}{Q_0} \right| = 0.933 \frac{E_1}{\delta \sqrt{I^2 - 1}}. \quad (2)$$

where,  $Q_0$  (in  $eb$ ) is the intrinsic quadrupole moment. Typical values for nuclei in the  $A \sim 180$  region are  $g_R \approx 0.28$  and  $Q_0 \approx 7 eb$ . The  $g_K$  value for an orbital with the asymptotic Nilsson quantum numbers  $\Omega^\pi [Nn_z\Lambda]$  is estimated from the relation:

$$Kg_K = \sum (\Lambda g_\Lambda + 0.6 \Sigma g_\Sigma). \quad (3)$$

where  $\Lambda$  and  $\Sigma$  are the projections of the nucleon orbital and spin angular momenta, respectively, with  $\Omega = \Lambda \pm \Sigma$ . A typical spin quenching factor of 0.6 is used [20].

Measured  $|(g_K - g_R)/Q_0|$  values from various levels in the rotational bands built on the  $K^\pi=10^+$ ,  $11^-$ , and  $14^+$  states are plotted in Fig. 10 and listed in Table II. It is evident that these values are in good agreement with those expected for the proposed configurations discussed hereafter. The additivity of excitation energies of different two-quasiparticle states required to realize corresponding four-quasiparticle excitations is evident in the following comparison. The  $K^\pi=4^-$  and  $K^\pi=8^-$  states are built on the  $\nu^2[624]9/2^+ \otimes [510]1/2^-$  and  $\pi^2[514]9/2^- \otimes [404]7/2^+$  configurations, respectively (Table III). The sum of excitation energies of the  $K^\pi=4^-$  and  $K^\pi=8^-$  isomers is 2515 keV, very close to the 2484-keV observed excitation energy of the  $K^\pi=12^+$  state, resulting from the  $\pi^2(8^-) \otimes \nu^2(4^-)$  configuration. Similarly, the sum of energies of the  $K^\pi=8^-$  and  $K^\pi=10^+$  states is 3565 keV and compares well with the excitation energy of the  $K^\pi=18^-$  state (3595 keV), resulting from the proposed  $\pi^2(8^-) \otimes \nu^2(10^+)$  configuration. Further, the  $K^\pi=14^+$  state at 2805 keV may be realized from the  $K^\pi=8^-$  and  $K^\pi=6^-$  ( $\nu^2[624]9/2 \otimes [512]3/2$ ) configurations, with the sum of the two energies being 2830 keV, close to the observed value of 2805 keV. The  $K^\pi=6^-$  state had been reported earlier from  $^{179}\text{Hf}(d,p)$  data [21]. Additionally, the following configurations are proposed. The  $K^\pi=10^+$  state is assigned a  $\nu^2[624]9/2 \otimes [615]11/2$  configuration, while a  $\pi^2[514]9/2$ ,  $[404]7/2 \otimes \nu^2[512]5/2$ ,  $[510]1/2$  is proposed for the  $K^\pi=11^-$  level. It is not possible to test the additivity of 2-quasiparticle energies for this  $K^\pi=11^-$  configuration since the excitation energy of the  $\nu^2[512]5/2$ ,  $[510]1/2$ :  $K^\pi=3^+$  state is not known.

The bands built on the  $K^\pi=8^+$  states in the  $N=106$  isotones  $^{180}\text{W}$  [22] and  $^{182}\text{Os}$  [23], and those built on the  $K^\pi=10^+$  levels in the  $N=108$  isotones *viz.*  $^{182}\text{W}$  [24] and  $^{184}\text{Os}$  [25] have been ascribed a so-called Fermi-aligned (or *t*-band) nature [26]. The term “*t*-band” stems from the description of such structures within the framework of the cranking model, where tilting of the cranking axis is required. In W and Os isotopes, the Fermi-aligned *t*-bands with  $\nu(i_{13/2})^2$  high- $K$  coupling cross the respective ground-state bands and become yrast at high spins, in contrast with the more usual scenario where a rotation-aligned *s* band with low- $K$  coupling is observed [22].

In  $^{180}\text{Hf}$ , unlike the case in the isotones  $^{182}\text{W}$  and  $^{184}\text{Os}$ , the  $K^\pi=10^+$  structure does not appear to exhibit the characteristics of a Fermi-aligned band. There are no transitions observed linking the  $K^\pi=10^+$  and the ground-state bands in  $^{180}\text{Hf}$ . Further, a plot of level



energies (with a rigid rotor reference subtracted) does not reveal any apparent interaction between the  $K^\pi=10^+$  and the ground-state band in  $^{180}\text{Hf}$ , in contrast to the situation in the two isotones, where it is visible through a change in the trajectory of the excitation energies as a function of spin (Fig. 11). This aspect is even more clearly evident in the  $N=106$  isotones  $^{180}\text{W}$  and  $^{182}\text{Os}$  (Fig. 12), where the  $K^\pi=8^+$  rotational sequences clearly cross the ground-state band and become yrast at high spins. The absence of  $t$ -bands in Hf isotopes could possibly be related to the rigidity of the prolate deformation with respect to the  $\gamma$  degree of freedom, which likely precludes an alignment along an axis intermediate between the symmetry and collective rotation ones.

The properties of high- $K$  states in  $^{180}\text{Hf}$  have been computed using multi-quasiparticle calculations, as described in Refs. [17, 27]. Specifically, single-particle energies were determined using the Nilsson potential with parameters  $\kappa$  and  $\mu$  adopted from Ref. [28], and equilibrium deformations,  $\epsilon_2$  and  $\epsilon_4$  from Ref. [29]. The states close to the proton and neutron Fermi surfaces were adjusted to reproduce approximately the experimental one-quasiparticle energies in the neighboring  $^{181}\text{Hf}$  (for neutrons) and  $^{181}\text{Ta}$  (for protons) odd-mass nuclei. The energies of multi-quasiparticle states were then calculated self-consistently by taking into account pairing using the Lipkin-Nogami prescription, with blocking and particle number conservation included [30]. Fixed pairing strengths of  $G_\nu=18/A$  and  $G_\pi=23.4/A$  were used, which, on average, reproduce the pairing gaps in the region [31]. The calculated energies were subsequently corrected for the effect of orbital-dependent residual nucleon-nucleon interactions with the approach outlined in Ref. [32] with updated Gallagher-Moszkowski splitting energies taken from Ref. [33].

A detailed comparison between experimental and calculated multi-quasiparticle states in  $^{180}\text{Hf}$  is given in Table III. The predicted energies for all two- and four-quasiparticle states are in fair agreement (within 200 keV) with the experimental values (Table III). Most of the low-lying, high- $K$  states predicted below 4 MeV have been observed in the experiment. It is worthwhile to contrast the  $K^\pi=16^+$  states in  $^{178}\text{Hf}$  and  $^{180}\text{Hf}$ . In both isotopes, the  $\pi^2(8^-)$  configuration is near-yrast ( $E_x \approx 1.1$  MeV). The  $\nu^2(8^-)$  configuration in  $^{178}\text{Hf}$  is around 1 MeV lower in energy as compared to the corresponding one in  $^{180}\text{Hf}$ . As a result, the  $K^\pi=16^+$  state in  $^{178}\text{Hf}$ , realized from the  $\nu^2(8^-) \otimes \pi^2(8^-)$  configuration, becomes deeply yrast, and all possible decay paths from this level involve a large change in  $K$  value leading to the longest half-life ( $T_{1/2}=31$  y) observed for any  $K$  isomer. In contrast, for both the  $K^\pi=16^+$

states observed in  $^{180}\text{Hf}$ , decays to levels in the rotational sequence built on the  $K^\pi=14^+$  state, with small or no  $K$  hindrance, are possible and no isomeric character is observed for either of the  $K^\pi=16^+$  levels in this nucleus as a result.

## V. SUMMARY

High- $K$ , multi-quasiparticle states and associated rotational sequences have been studied in  $^{180}\text{Hf}$ . Two- and four-quasiparticle states up to 3.6 MeV have been identified, and these become increasingly favored in energy at higher excitation. The lifetimes of several  $K$ -isomeric levels, ranging from  $\approx 1$  ns to 1  $\mu$ s, were determined, and some half-lives reported earlier have been modified. Decay hindrances deduced from the data indicate that the  $K$  quantum number is robust for most of the isomeric decays. Configuration assignments for the observed high- $K$  structures have been proposed based on branching ratios from corresponding rotational sequences. The  $K^\pi=10^+$  structure in  $^{180}\text{Hf}$  does not appear to have a Fermi-aligned character, unlike the situation in the W and Os isotones. Multi-quasiparticle calculations employing the Lipkin-Nogami prescription for pairing, with blocking and particle number conservation included, provide a satisfactory description of the excitation energies of high- $K$  states determined by the experiment. With the increase in excitation, high- $K$  states are predicted to be even more favored, and experiments optimized for populating higher spin levels and measuring longer half-lives are expected to reveal their presence.

## ACKNOWLEDGMENTS

This work is supported by the U.S. Department of Energy, Office of Science, Office of Nuclear Physics, under award numbers DE-FG02-94ER40848 and DE-FG02-94ER40834, and contract number DE-AC02-06CH11357. The research described here utilized resources of the ATLAS facility at ANL, which is a DOE Office of Science user facility. The authors thank the ATLAS crew for providing a sustained, stable beam for the entire duration of the

experiment.

- 
- [1] K. Brandi, R. Engelmann, V. Hepp, E. Kluge, H. Krehbiel, U. Meyer-Berkhout, Nucl. Phys. **59**, 33 (1964).
  - [2] T. L. Khoo, F. M. Bernthal, R. A. Warner, G. F. Bertsch, and G. Hamilton, Phys. Rev. Lett. **35**, 1256 (1975).
  - [3] P.M. Walker, D.M. Cullen, C.S. Purry, D.E. Appelbe, A.P. Byrne, G.D. Dracoulis, T. Kibedi, F.G. Kondev, I.Y. Lee, A.O. Macchiavelli, A.T. Reed, P.H. Regan, F. Xu, Phys. Lett. B **408**, 42 (1997).
  - [4] G. D. Dracoulis, F. G. Kondev, G. J. Lane, A. P. Byrne, T. R. McGoram, T. Kibedi, I. Ahmad, M. P. Carpenter, R. V. F. Janssens, T. Lauritsen, C. J. Lister, D. Seweryniak, P. Chowdhury, and S. K. Tandel, Phys. Rev. Lett. **97**, 122501 (2006).
  - [5] P. Chowdhury, B. Fabricius, C. Christensen, F. Azgui, S. Bjornholm, J. Borggreen, A. Holm, J. Pedersen, G. Sletten, M.A. Bentley, D. Howe, A.R. Mokhtar, J.D. Morrison, J.F. Sharpey-Schafer, P.M. Walker, R.M. Lieder, Nucl. Phys. A **485**, 136 (1988).
  - [6] S. K. Tandel, P. Chowdhury, E. H. Seabury, I. Ahmad, M. P. Carpenter, S. M. Fischer, R. V. F. Janssens, T. L. Khoo, T. Lauritsen, C. J. Lister, D. Seweryniak, Y. R. Shimizu, Phys. Rev. C **73**, 044306 (2006); S. K. Tandel, A. J. Knox, C. Parnell-Lampen, U. S. Tandel, P. Chowdhury, M. P. Carpenter, R. V. F. Janssens, T. L. Khoo, T. Lauritsen, C. J. Lister, D. Seweryniak, X. Wang, S. Zhu, D. J. Hartley, Jing-ye Zhang, Phys. Rev. C **77**, 024313 (2008).
  - [7] S. B. Burson, K. W. Blair, H. B. Keller, S. Wexler, Phys. Rev. **83**, 62 (1951).
  - [8] R. D'Alarcao, P. Chowdhury, E. H. Seabury, P. M. Walker, C. Wheldon, I. Ahmad, M. P. Carpenter, G. Hackman, R. V. F. Janssens, T. L. Khoo, C. J. Lister, D. Nisius, P. Reiter, D. Seweryniak, I. Wiedenhoever, Phys. Rev. C **59**, R1227 (1999).
  - [9] I-Yang Lee, Nucl. Phys. A **520**, c641 (1990).
  - [10] R.V.F. Janssens and F.S. Stephens, Nucl. Phys. News **6**, 9 (1996).
  - [11] E. Ngijoi-Yogo, S. K. Tandel, G. Mukherjee, I. Shestakova, P. Chowdhury, C. Y. Wu, D. Cline, A. B. Hayes, R. Teng, R. M. Clark, P. Fallon, A. O. Macchiavelli, K. Vetter, F. G. Kondev, S. Langdown, P. M. Walker, C. Wheldon, and D. M. Cullen, Phys. Rev. C **75**, 034305 (2007).

- [12] U. S. Tandel, S. K. Tandel, P. Chowdhury, D. Cline, C. Y. Wu, M. P. Carpenter, R. V. F. Janssens, T. L. Khoo, T. Lauritsen, C. J. Lister, D. Seweryniak, S. Zhu, Phys. Rev. Lett. **101**, 182503 (2008).
- [13] M.W. Simon, D. Cline, C.Y. Wu, R.W. Gray, R. Teng, C. Long, Nucl. Instr. and Meth. in Phys. Res. A **452**, 205 (2000).
- [14] E.A. McCutchan, Nuclear Data Sheets **126** (2015) 151.
- [15] W. Andrejtscheff, M. Senba, N. Tsoupas, Z.Z. Ding, Nucl. Inst. and Meth. in Phys. Res. **204** (1982) 123.
- [16] S. M. Mullins, G. D. Dracoulis, A. P. Byrne, T. R. McGoram, S. Bayer, R. A. Bark, R. T. Newman, W. A. Seale, F. G. Kondev, Phys. Rev. C **61**, 044315 (2000).
- [17] F.G. Kondev, G.D. Dracoulis, A.P. Byrne, T. Kibedi, Nucl.Phys. A **632**, 473 (1998).
- [18] T.L.Khoo, J.C.Waddington, M.W.Johns, Can. J. Phys. **51**, 153 (1973).
- [19] F.G. Kondev, G.D. Dracoulis, T. Kibedi, At. Data and Nucl. Data Tables **103-104** (2015) 50.
- [20] P. M. Walker, G. D. Dracoulis, A. P. Byrne, B. Fabricius, T. Kibedi, and A. E. Stuchbery, Nucl. Phys. A **568** (1994) 397.
- [21] J. I. Zaitz and R. K. Sheline, Phys. Rev. C **75**, 034305 (2007).
- [22] P.M. Walker, K.C. Yeung, G.D. Dracoulis, P.H. Regan, G.J. Lane, P.M. Davidson, A.E. Stuchbery, Phys. Lett. B **309**, 17 (1993).
- [23] T. Kutsarova, R.M. Lieder, H. Schnare, G. Hebbinghaus, D. Balabanski, W. Gast, A. Kramer-Flecken, M.A. Bentley, P. Fallon, D. Howe, A.R. Mokhtar, J.F. Sharpey-Schafer, P. Walker, P. Chowdhury, B. Fabricius, G. Sletten, S. Frauendorf, Nucl.Phys. A **587**, 111 (1995).
- [24] T. Shizuma, S. Mitarai, G. Sletten, R.A. Bark, N.L. Gjorup, H.J. Jensen, J. Wrzesinski, M. Piiparinen, Nucl.Phys. A **593**, 247 (1995).
- [25] T. Shizuma, K. Matsuura, T. Jumatsu, K. Hata, Y. Sasaki, H. Ishiyama, M. Kato, K. Uchiyama, T. Komatsubara, K. Furuno, T. Hayakawa, Phys. Lett. B **442**, 53 (1998).
- [26] P. M. Walker, G. D. Dracoulis, A. P. Byrne, B. Fabricius, T. Kibedi, and A. E. Stuchbery, Phys. Rev. Lett. **67**, 433 (1991).
- [27] F.G. Kondev, G.D. Dracoulis, A.P. Byrne, T. Kibedi, S. Bayer, Nucl.Phys. A **617**, 91 (1997).
- [28] Tord Bengtsson and Ingemar Ragnarsson, Nucl. Phys. A **436**, 14 (1985).
- [29] P. Moller, J.R. Nix, W.D. Myers, W.J. Swiatecki, At. Data and Nucl. Data Tables **59**, 185 (1995).

- [30] W. Nazarewicz, M.A. Riley, J.D. Garrett, Nucl. Phys. A **512**, 61 (1990).
- [31] G. Audi, W. Mang, A.H. Wapstra, F.G. Kondev, M. MacCormick, X. Xu, B. Pfeiffer, Chin. Phys. C **36**, 1603 (2012).
- [32] K. Jain, O. Burgh, G.D. Dracoulis, B. Fabricius, P.M. Walker, N. Rowley, Nucl. Phys. A **591**, 61 (1994).
- [33] F.G. Kondev, PhD Thesis, Australian National University, 1997, unpublished.
- [34] T. Kibedi, T.W. Burrows, M.B. Trzhaskovskaya, P.M. Davidson, C.W. Nestor, Jr., Nucl. Instr. and Meth. A **589** (2008) 202.

TABLE I: Decay of high- $K$  isomers in  $^{180}\text{Hf}$ . The spin-parity, half-life and excitation energy of high- $K$  states is listed. Energy, multipolarity and relative intensity of transitions deexciting these states along with corresponding reduced hindrances are also tabulated. Values from Ref [19] are adopted for the  $K^\pi=8^-$  isomer. Theoretical conversion coefficients (Ref [34]) are used where experimental data are not available.

$K^\pi$	$T_{1/2}$	$E_x$ (keV)	$E_\gamma$ (keV)	Multipolarity	$I_\gamma$	$f_\nu$
$4^-$	$0.52(8) \mu\text{s}$	1374	1066	$E1$	100(1)	1446(22)
			1281	$M2$	4.5(2)	205(7)
$6^+$	$2.8(3) \text{ ns}$	1702	1062	$M1$	78(5)	12.8(3)
			1394	$E2$	100(5)	7.3(2)
$8^-$	$5.53(2) \text{ h}$	1141	58	$E1$	100.0(4)	224.4(3)
			501	$M2$	29.8(6)	216(3)
			501	$E3$	29.8(6)	67.3(3)
$10^+$	$< 2 \text{ ns}$	2424	479	$E1$	7.2(7)	$\leq 1.7\text{E}+7$
			772	$E1$	13.0(13)	$\leq 4.0\text{E}+7$
			1040	$E1$	100(10)	$\leq 1.3\text{E}+7$
$12^+$	$0.94(11) \mu\text{s}$	2484	222	$E1$	2.7(3)	$1.33(8)\text{E}+3$
			539	$E1$	100(10)	960(40)
			832	$M2$	4.0(4)	112(10)
			1100	$E3$	21.0(21)	18(3)
$(18^-)$	$> 1 \mu\text{s}$	3595	(69)	$(M2)$	1.3(3)	
			151	$(M2)$	100(10)	

TABLE II: Proposed configuration assignments for new high- $K$  bands in  $^{180}\text{Hf}$

$K^\pi$	Configuration		$\frac{q_K - q_R}{Q_0}$	$\left  \frac{q_K - q_R}{Q_0} \right $
	$\nu$	$\pi$	Expected	Experiment
$10^+$	[624]9/2 [615]11/2		0.072	0.067(6)
$11^-$	[512]5/2 [510]1/2	[514]9/2 [404]7/2	0.034	0.036(8)
$14^+$	[624]9/2 [512]3/2	[514]9/2 [404]7/2	0.042	0.045(6)

TABLE III: Calculated and experimental multi-quasiparticle states in  $^{180}\text{Hf}$

$K^\pi$	Configuration		$E_{qp}$	$E_{res}$	$E_{calc}$	$E_{exp}$
	$\nu$	$\pi$	(keV)	(keV)	(keV)	(keV)
$4^-$	$1/2^-, \mathbf{9/2^+}$		1494	-150	1344	1374
$8^-$		$7/2^+, 9/2^-$	1187	-150	1037	1141
$10^+$	$\mathbf{9/2^+}, \mathbf{11/2^+}$		2163	+200	2363	2424
$12^+$	$1/2^-, \mathbf{9/2^+}$	$7/2^+, 9/2^-$	2680	-258	2422	2484
$12^-$	$1/2^-, 7/2^-$	$7/2^+, 9/2^-$	2951	-409	2542	
$13^+$	$1/2^-, \mathbf{9/2^+}$	$7/2^+, 9/2^-$	2680	0	2680	2535
$14^+$	$3/2^-, \mathbf{9/2^+}$	$7/2^+, 9/2^-$	2964	-255	2710	2805
$16^+$	$7/2^-, \mathbf{9/2^+}$	$7/2^+, 9/2^-$	3594	-300	3295	3444
$16^+$	$7/2^-, \mathbf{9/2^+}$	$7/2^+, 9/2^-$	3389	10	3399	3526
$18^-$	$\mathbf{9/2^+}, \mathbf{11/2^+}$	$7/2^+, 9/2^-$	3349	-8	3341	3595

Configurations: **Neutrons** ( $\nu$ ):  $1/2^-$ :  $1/2^-$ [510];  $3/2^-$ :  $3/2^-$ [512];  $\mathbf{9/2^+}$ :  $9/2^+$ [624];  $\mathbf{11/2^+}$ :

$11/2^+$ [615];  $5/2^-$ :  $5/2^-$ [512];  $7/2^-$ :  $7/2^-$ [514];  $7/2^-$ :  $7/2^-$ [503].

**Protons** ( $\pi$ ):  $9/2^-$ :  $9/2^-$ [514];  $7/2^+$ :  $7/2^+$ [404];  $5/2^+$ :  $5/2^+$ [402].



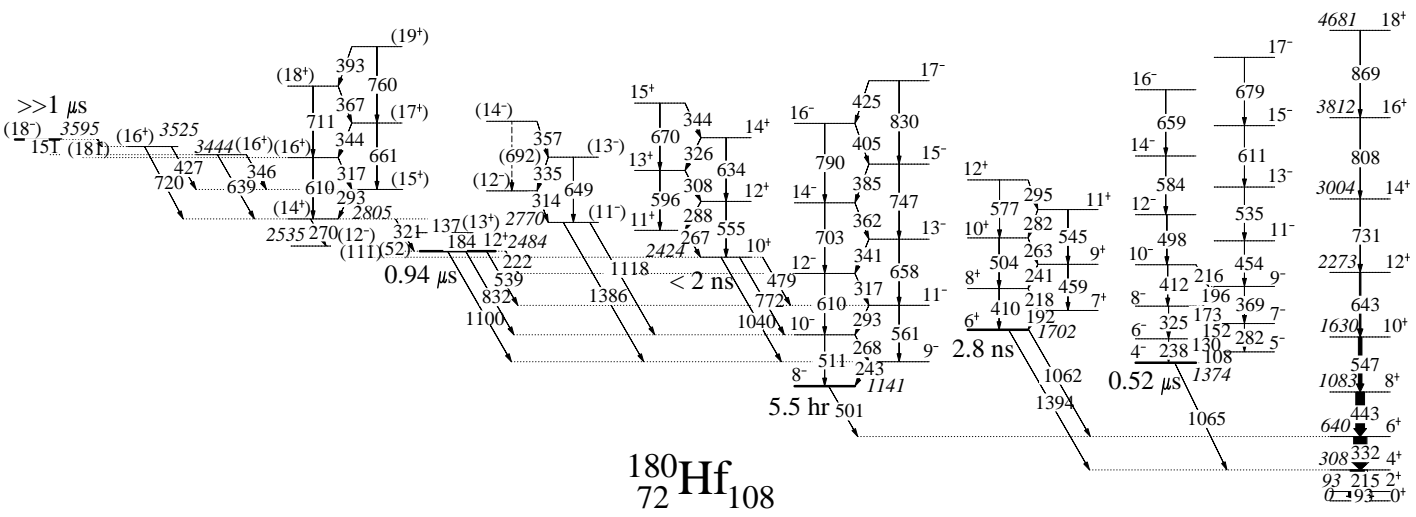


FIG. 1: Decay scheme illustrating high- $K$  structures in  $^{180}\text{Hf}$ . The half-lives of the  $K$  isomers or the established limits are also indicated.

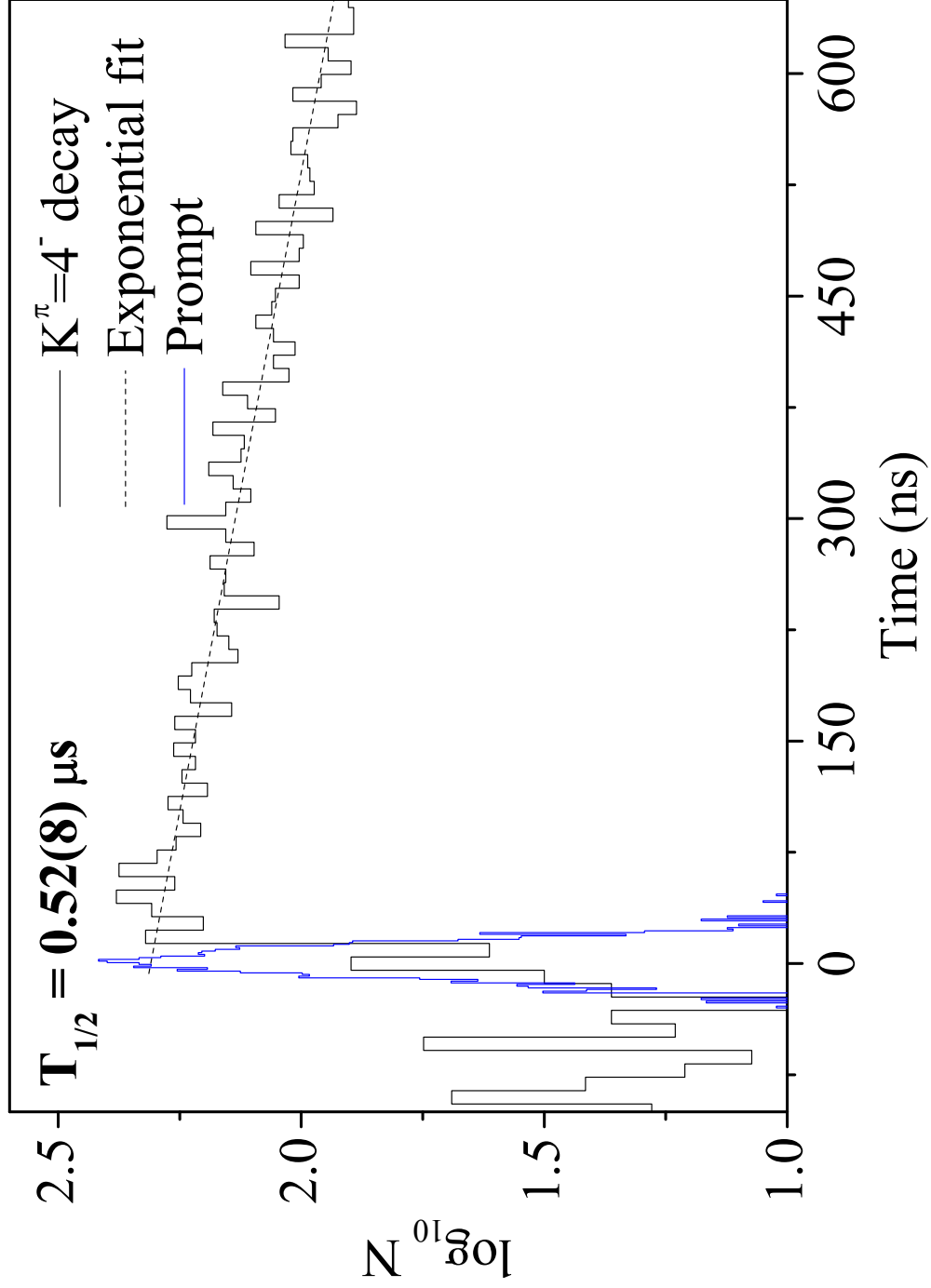


FIG. 2: (Color online) Time difference spectrum between transitions feeding (238 and 325 keV) and deexciting (1066 keV) the  $K^{\pi}=4^{-}$  isomeric state. A half-life of  $0.52(8) \mu s$  is deduced. The time distribution for prompt transitions is presented for comparison.

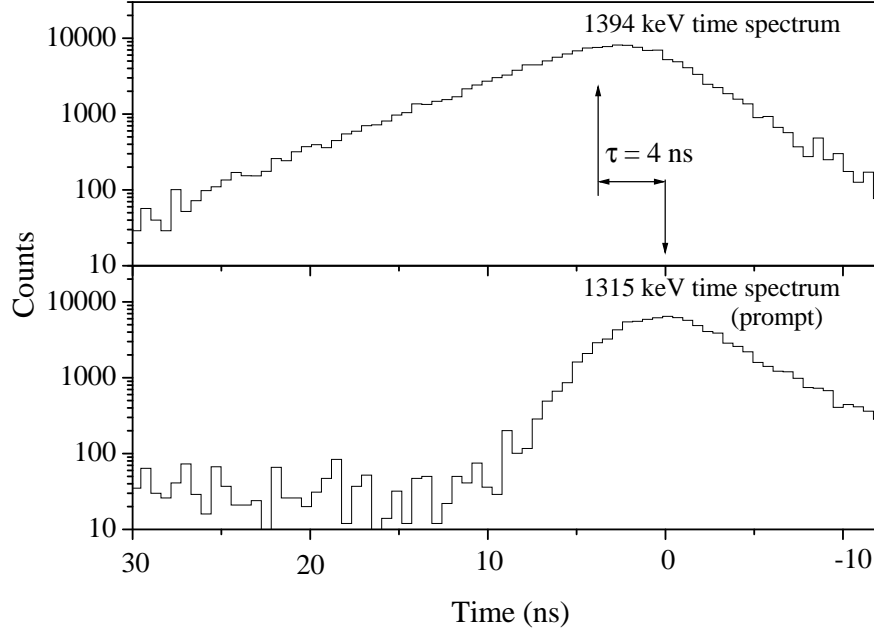


FIG. 3: Centroids in the time distribution of the 1394-keV transition deexciting the  $K^\pi=4^-$  state. The centroid of the 1315-keV transition from a prompt state is given for comparison.

A distinct shift of 4 *ns* is evident for the 1394-keV transition. See text for details.

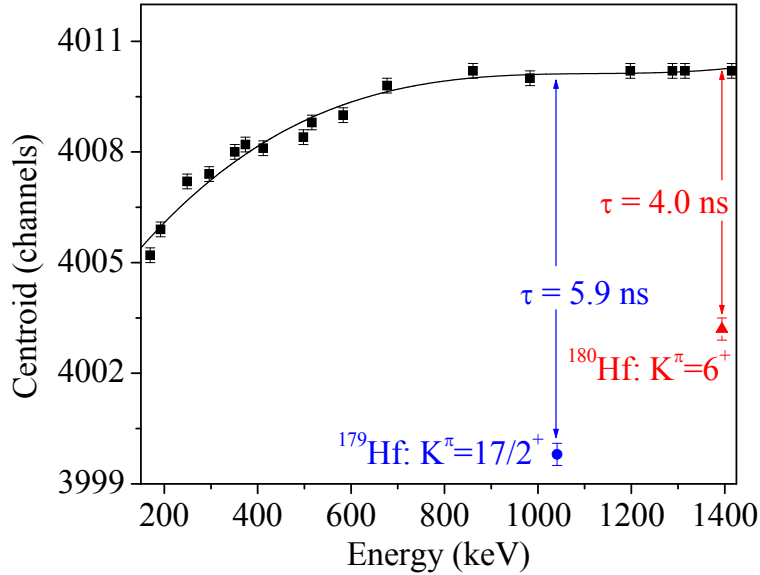


FIG. 4: (Color online) The variation of the centroid of the time distributions as a function of energy for prompt transitions. In the case of transitions from isomeric states in  $^{179,180}\text{Hf}$  (colored points), considerable shifts in the centroids are clearly visible.

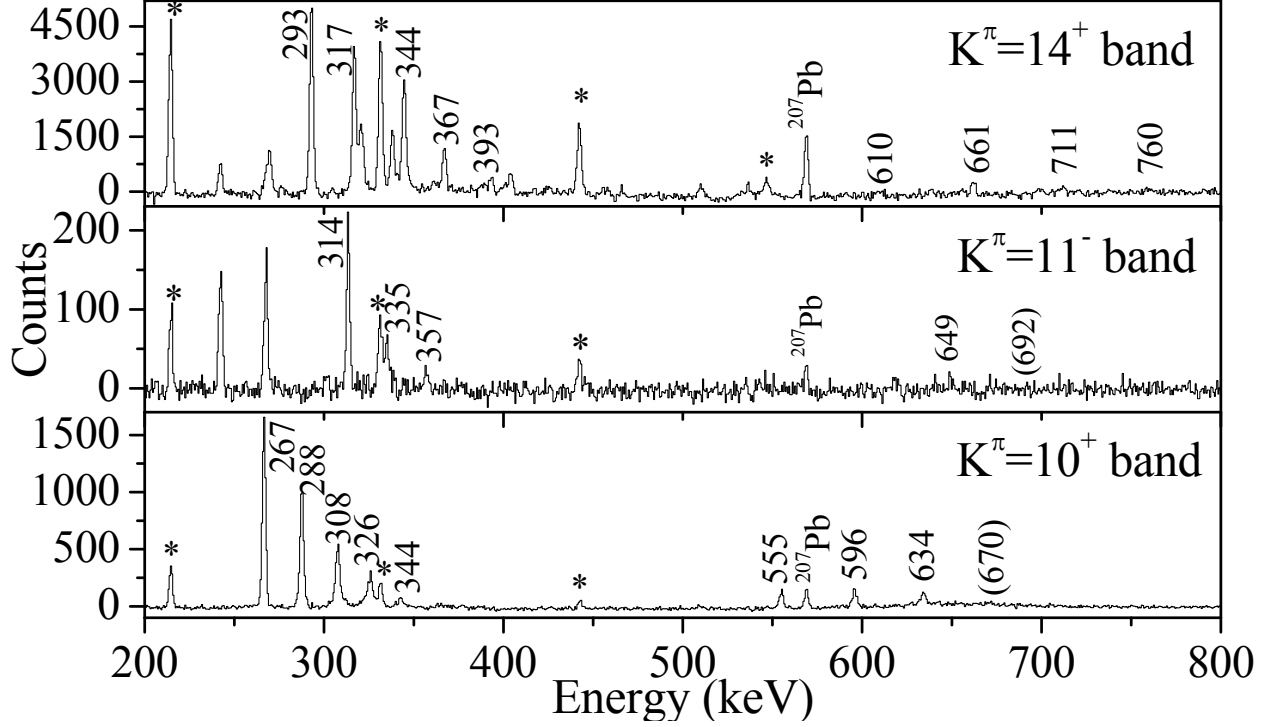


FIG. 5: Gated spectra illustrating transitions in rotational bands built on the  $K^\pi=10^+$ ,  $11^-$  and  $14^+$  states.  $\Delta I=1$  transitions are below 400 keV, and  $\Delta I=2$   $\gamma$  rays above 500 keV.

Transitions from the ground-state band in  $^{180}\text{Hf}$ , present due to random coincidence events, are marked with asterisks. Additional transitions in the spectra are visible through coincidences with  $\gamma$  rays from other structures in  $^{180}\text{Hf}$ . The 569-keV transition in  $^{207}\text{Pb}$  (beam) is visible through cross coincidence. The spectrum for the  $K^\pi=10^+$  sequence is obtained by means of a double coincidence gate on the 243- and 1040-keV transitions, while that for the  $K^\pi=11^-$  band is obtained by summing double gates on 1118-keV with 243- and 268-keV transitions, respectively. The  $K^\pi=14^+$  spectrum is obtained by summing double coincidence gates on inband transitions and ones deexciting the band-head state.

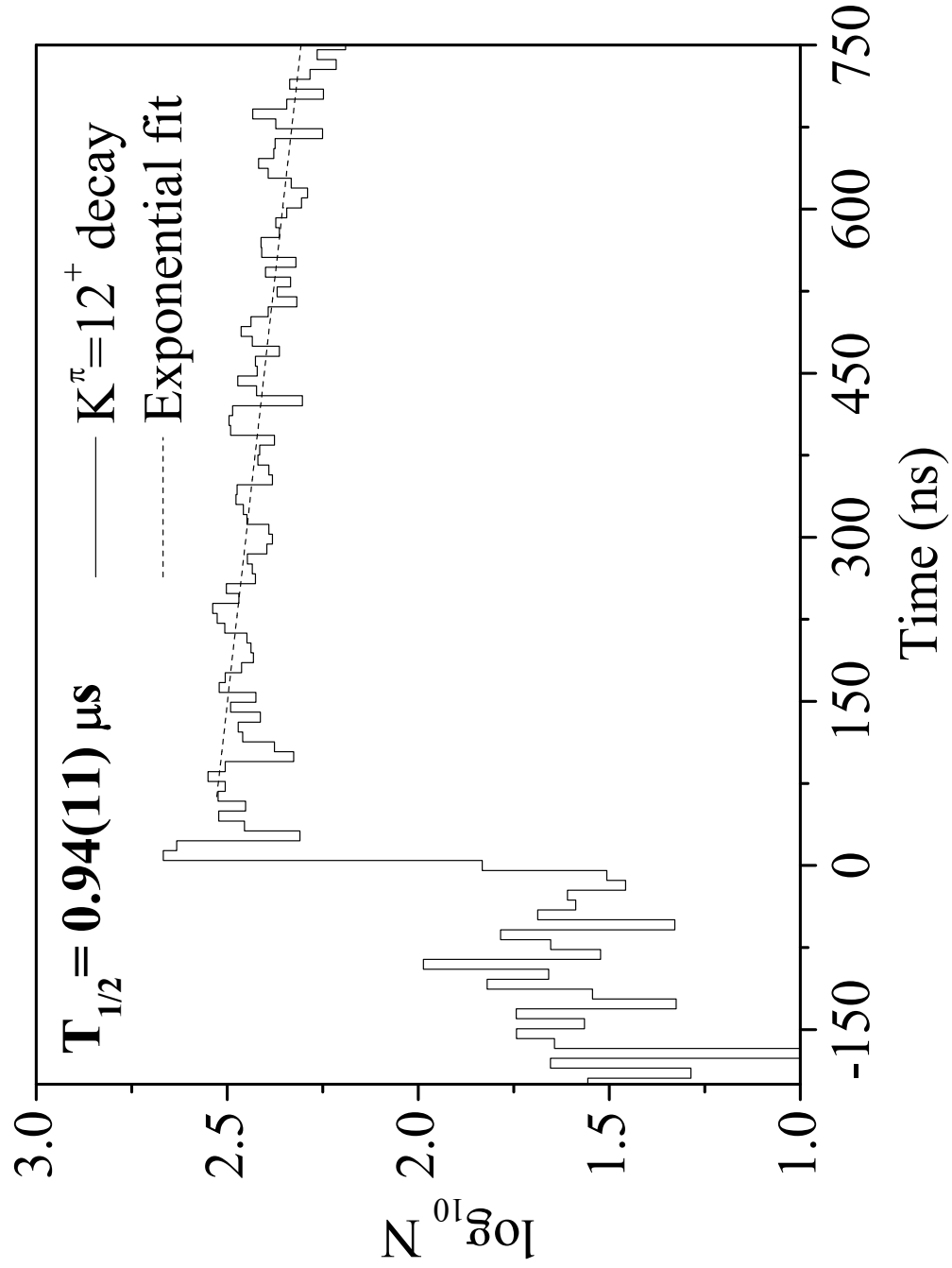


FIG. 6: Time difference spectrum between transitions feeding (184 and 321 keV) and deexciting (539 keV) the  $K^\pi=12^+$  isomeric state. A half-life of  $0.94(11) \mu s$  is deduced.

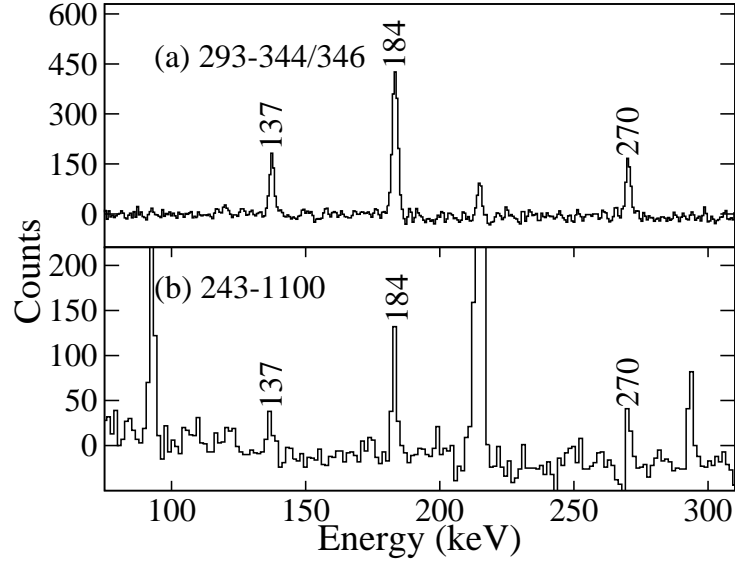


FIG. 7: Comparison of relative intensities of 137-, 184- and 270-keV  $\gamma$  rays with gates on transitions: (a) above the  $K^\pi=14^+$  level, and (b) below the  $K^\pi=12^+$  state. The similarity of the ratio of relative intensities of the 270-keV  $\gamma$  ray with the 137- and 184-keV transitions in the two spectra preclude the long-lived ( $T_{1/2} \gg 10 \mu\text{s}$ ) isomeric character reported earlier [8] for the level at 2535 keV, and suggest  $T_{1/2} \ll 1 \mu\text{s}$ .

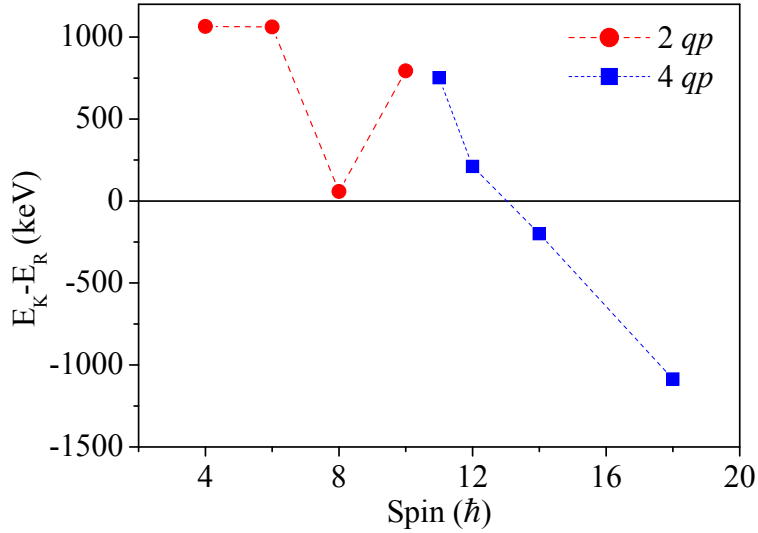


FIG. 8: (Color online) Variation with spin of the difference between excitation energies of high- $K$  states and yrast collective rotational levels in  $^{180}\text{Hf}$ .

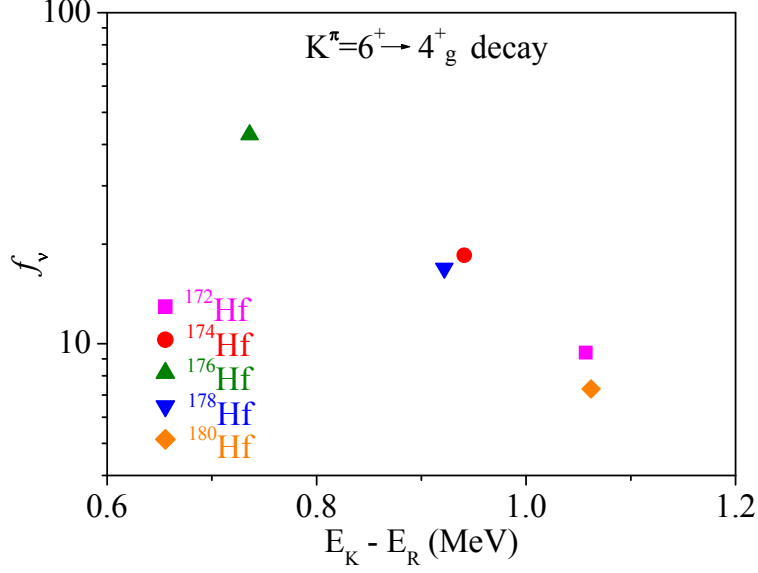


FIG. 9: (Color online) Reduced hindrances ( $f_\nu$ ) for decays from  $K^\pi=6^+$  isomers to the  $4^+$  state in the ground-state band of even Hf isotopes. The hindrance is most pronounced in the case of  $^{176}\text{Hf}$ , where the configuration is lowest in energy, and decreases towards the neutron- and proton-rich sides. In all cases, the uncertainties in reduced hindrances are quite small, and therefore not visible outside the symbols.

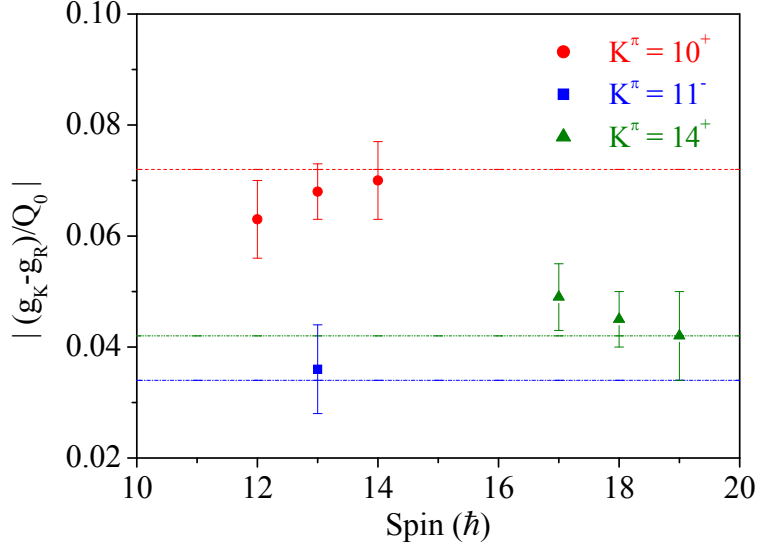


FIG. 10: (Color online) Values of  $|(g_K - g_R)/Q_0|$  as a function of spin for  $K^\pi=10^+$ ,  $11^-$ , and  $14^+$  configurations in  $^{180}\text{Hf}$ . Measured values, obtained from branching ratios as described in the text, are displayed along with expected values (dotted lines).

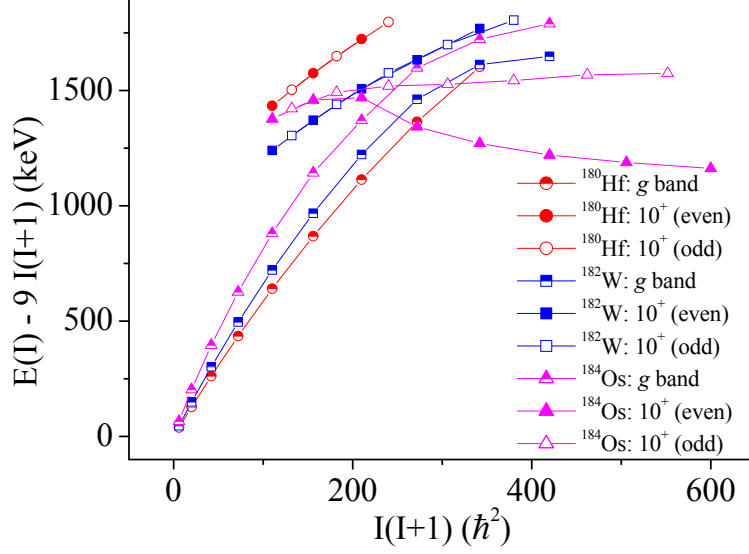


FIG. 11: (Color online) Excitation energies, with a rigid rotor reference subtracted as indicated, as a function of spin for the yrast positive-parity states, and bands built on the  $10^+$  states (both even and odd spin) in Hf, W and Os isotones with  $N=108$ .

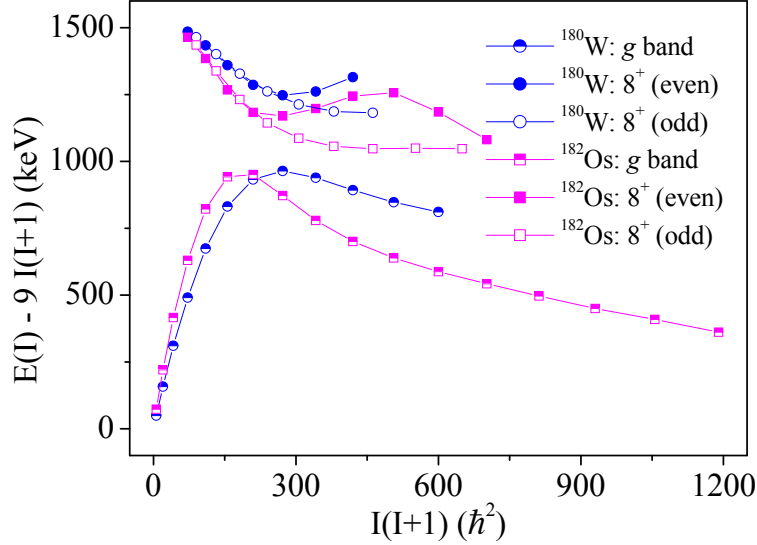


FIG. 12: (Color online) Excitation energies, with a rigid rotor reference subtracted, as a function of spin for the yrast positive-parity states, and bands built on the  $8^+$  states (both even and odd spin) in W and Os isotones with  $N=106$ .